# Modeling of maize gross primary production using MODIS imagery and flux tower data

Li Shihua[1*], He Ping[1], Liu Baosheng[1], Ni Ping[1], Han Xing[2]

(1. *School of Resources and Environment, University of Electronic Science and Technology of China, Chengdu 611731, China*; 2. *School of Resources and Environment, Jilin Agricultural University, Changchun 130018, China*)

**Abstract:** Maize is one of the most important crops cultivated on the global scale. Accurate estimation of maize Gross Primary Production (GPP) can provide valuable information for regional and global carbon budget studies. From site level to regional/global scales, GPP estimation depends on remote sensing or eddy covariance flux data. In this research, the 8-day composite GPP of maize was estimated by Moderate Resolution Imaging Spectroradiometer (MODIS) and flux tower data at eight study sites using a Regional Production Efficiency Model (REG-PEM). The performance of the model was assessed by analyzing the linearly regression of GPP estimated from the REG-PEM model ($GPP_{EST}$) with the GPP predicted from the eddy covariance data ($GPP_{EC}$). The coefficient of determination, root mean squared error and mean absolute error of the regression model were calculated. The uncertainties of the model are also discussed in this research. The seasonal dynamics (phases and magnitudes) of the $GPP_{EST}$ reasonably agreed with those of $GPP_{EC}$, indicating the potential of the satellite-driven REG-PEM model for up-scaling the GPP in maize croplands. Furthermore, the maize GPP estimated by this model is more accurate than the MODIS GPP products (MOD17A2). In particular, MOD17A2 significantly underestimated the GPP of maize croplands. The uncertainties in the REG-PEM model are mostly contributed by the maximum light use efficiency and the fraction of photosynthetically active radiation.

**Keywords:** gross primary production, maize, light use efficiency, MODIS, remote sensing, flux data

**DOI:** 10.3965/j.ijabe.20160902.2245

**Citation:** Li S H, He P, Liu B S, Ni P, Han X. Modeling of maize gross primary production using MODIS imagery and flux tower data. Int J Agric & Biol Eng, 2016; 9(2): 110－118.

## 1 Introduction

Crops constitute the most pervasive anthropogenic biome in the world[1]. Cropland covers approximately 24% of the Earth's land surface[2]. The energy balance between the biosphere and atmosphere is analyzed through the Gross Primary Production (GPP), defined as the overall rate of carbon fixation through photosynthetic processes in vegetation[3-5]. The GPP is potentially useful for estimating crop yield and carbon budgets[6,7]. An accurate and synoptic quantification of the spatial and temporal distributions of crop GPP is essential for crop growth and carbon exchange monitoring[8,9]. Maize is a main food for the world's human population, and there is a growing interest in regional-scale estimation of maize GPP.

Satellite remote sensing is a powerful and expedient tool for assessing GPP at regional and global scales[10]. Maize GPP has been estimated by Landsat Enhanced Thematic Mapper plus (ETM+)[1,9] and the Moderate Resolution Imaging Spectroradiometer (MODIS)[5,8,10-12,15-19]. The first method predicts the maize GPP from the chlorophyll index. Sakamoto et al.[11] developed the MODIS Wide Dynamic Range

**Received date:** 2015-11-20 **Accepted date:** 2016-03-08

**Biographies: He Ping,** Master candidate, research interest: agricultural remote sensing, Email: 1508556267@qq.com; **Liu Baosheng**, Master, research interest: global change remote sensing. Email: sdhzlbs@163.com; **Ni Ping**, Master, research interest: agricultural remote sensing, Email: 455836324@qq.com; **Han Xing**, Master, research interest: agricultural remote sensing, Email: jlndhx@126.com.

* **Corresponding author: Li Shihua,** PhD, Associate Professor, research interest: remote sensing and its applications in agriculture and global change. Mailing address: No.2006, Xiyuan Ave, West Hi-Tech Zone, School of Resources and Environment, University of Electronic Science and Technology of China, Chengdu, 611731, China. Email: lishihua@uestc.edu.cn.

Vegetation Index (WDRVI) for quantifying the daily GPP of maize from shortwave radiation data; Wu et al.[5] used the green Chlorophyll Index ($CI_{green}$) to estimate the GPP of maize and other plants; Peng et al.[8,12] compared the ability of several widely used chlorophyll-related vegetation indices to estimate the total chlorophyll content and GPP in maize. The second estimation method is the Light Use Efficiency (LUE) model, which can potentially estimate the spatial and temporal dynamics of GPP because of its theoretical basis and practicality[13,14]. Among the LUE models, the Vegetation Photosynthesis Model (VPM) has been used for GPP estimation in irrigated and rain-fed maize[15], a winter-wheat and maize double cropping system[16], maize cropland and degraded grassland in a semiarid area of Northeast China[17], and maize and alpine meadow GPP in the Heihe river basin (Northern China)[18]. Zhang et al.[19] examined the impacts of the MODIS observation footprint and the vegetation Bidirectional Reflectance Distribution Function (BRDF) on crop daily GPP estimation.

The seasonal and inter-annual dynamics of maize GPP in fields can be computed by tower eddy covariance systems[8]. The eddy covariance technique in the flux tower is an advanced micrometeorological method for estimating $CO_2$, water, and energy exchanges between the atmosphere and terrestrial ecosystems[20-21]. It directly measures the Net Ecosystem Exchange (NEE) of $CO_2$, providing a footprint related to the tower height, atmospheric stability, wind speed and direction. GPP can be calculated from daytime NEE and ecosystem respiration values from the flux data[18]. Tower eddy covariance systems have also been used for calibrating and evaluating LUE models[22].

The only global-scale operational GPP product with high temporal resolution is MODIS GPP product (MOD17A2), which is spatially and temporally resolved to 1 km and 8 days, respectively[22]. The biome type-specific maximum conversion efficiency is calculated from NASA's Global Modeling and Assimilation Office (GMAO) meteorological reanalysis data, and the Fraction of Photosynthetically Active Radiation (FPAR) product (MOD15A2) is based on the LUE concept[23,24]. However, the maize GPP in the MOD17A2 products is significantly lower than the GPP predicted from flux tower data[25-28]. Regional GPP has been successfully estimated by the Regional Production Efficiency Model (REG-PEM), which is based on LUE theory[29-31] and inputs only remote sensing data. The objectives of this research are: 1) to evaluate the performance of the REG-PEM model in maize GPP estimation using MODIS and flux tower data, and 2) to analyze the uncertainties in the REG-PEM model.

## 2 Data and methods

### 2.1 Study sites

The flux data were collected from eight maize croplands with eddy covariance towers. Six of the study sites are located in North America, one in Germany and one in China (Figure 1). The study sites are briefly described in Table 1, and detailed information can be found in the associated references. Sites US-Ne1, DE-Kli and YK are continuous maize cultivations; the other sites are rotated between maize and soybean cultivations. For these sites, we used only the years of maize cultivation in the maize GPP estimation. For example, at the US-Ne2 site, we employed the data of 2001 and 2003. The flux data at Yingke (YK) are available from the Watershed Allied Telemetry Experimental Research (WATER) project[36] (http://westdc.westgis.ac.cn/data). The other flux data were obtained from the FLUXNET website (http://fluxnet.ornl.gov/).

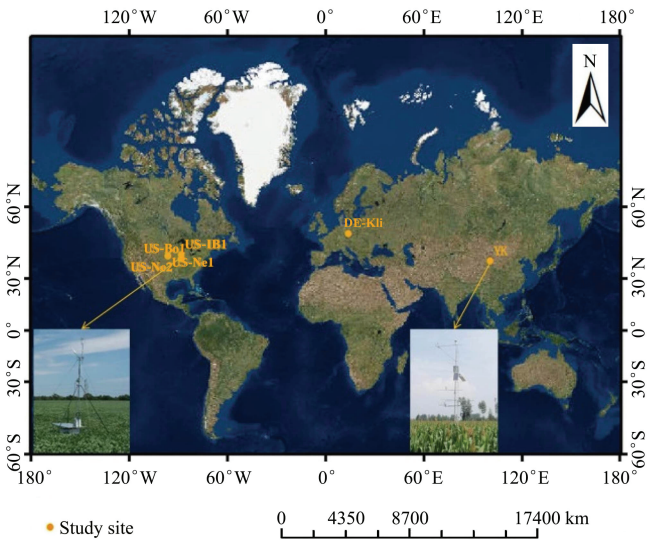


Figure 1 Locations of study sites

**Table 1 Characteristics of study sites**

| Site | Latitude, longitude | Altitude/m | Flux data | Reference |
|---|---|---|---|---|
| US-Ne1 | 41°09′54.2″N, 96°28′35.9″W | 361 | 2001-2004 | [32] |
| US-Ne2 | 41°09′53.5″N, 96°28′12.3″W | 362 | 2001, 2003 | [32] |
| US-Ne3 | 41°10′46.8″N, 96°26′22.7″W | 362 | 2001, 2003 | [32] |
| US-Bo1 | 40°00′22.3″N, 88°17′25.4″W | 218 | 2001, 2003, 2005 | [33] |
| US-Bo2 | 40°00′22″N, 88°17′30.5″W | 213 | 2004, 2006 | [34] |
| US-IB1 | 41°51′33.48″N, 88°13′21.72″W | 219 | 2006 | [35] |
| DE-Kli | 50°53′34.4″N, 13°31′21″E | 475 | 2005-2006 | [34] |
| Yingke (YK) | 38°51′25.7″N, 100°24′37.2″E | 1519 | 2008-2009 | [36] |

### 2.2 Remote sensing data

The MODIS surface reflectance product (MOD09) datasets (with spatial resolutions of 250 m and 500 m) and the MOD17A2 products at the geographic location of each flux tower were downloaded from the USGS EDC website. Based on the geo-location information of the study sites, the vegetation indices derived from the MOD09 products were extracted from 3×3 pixels located at the center of the flux tower at the study site. Using the surface reflectance ($\rho$) from the blue, red, near-infrared (NIR), and shortwave infrared (SWIR) bands, two vegetation indices were calculated: the enhanced vegetation index (EVI)[37] and the land surface water index (LSWI)[38, 39]:

$$EVI = G \times \frac{\rho_{nir} - \rho_{red}}{\rho_{nir} + (C_1 \times \rho_{red} - C_2 \times \rho_{blue}) + L} \quad (2)$$

$$LSWI = \frac{\rho_{nir} - \rho_{swir}}{\rho_{nir} + \rho_{swir}} \quad (3)$$

where, $\rho_{blue}$, $\rho_{red}$, $\rho_{nir}$, and $\rho_{swir}$ denote the reflectance of the MODIS blue, red, NIR and SWIR spectral bands, respectively; $L$ (=1) is the canopy background adjustment, $C_1$ (=6) and $C_2$ (=7.5) are aerosol resistance coefficients, and $G$ (=2.5) is the gain factor.

Time-series EVI data derived from satellite data typically contain noise from cloud contamination, atmospheric variability, and bidirectional reflectance[40,41]. Noise reduction or model fitting of the observed data is necessary before performing the GPP estimation. To reduce effects of cloud and other noise, the MODIS EVI time-series data were subjected to Harmonic ANalysis of Time Series (HANTS)[42,43]. Meanwhile, all the MOD09 data files have quality flags, including cloud and shadow flags.

### 2.3 Description of the REG-PEM model

The REG-PEM model described by Equation (4), which depends on the incident Photosynthetically Active Radiation (PAR) absorbed by the vegetation and the LUE ($\varepsilon$)[29-31]:

$$GPP = PAR \times FPAR \times \varepsilon \quad (4)$$

The FPAR is estimated as a linear function of EVI, and the coefficient $a$ is simply set to 1.0[38,39]:

$$FPAR = a \times EVI \quad (5)$$

The LUE is affected by the maximum possible efficiency of light, temperature and water:

$$\varepsilon = \varepsilon^* \cdot f(T) \cdot f(W) \quad (6)$$

where, $\varepsilon^*$ is the maximum possible efficiency (for a C4 plant, $\varepsilon^* = 2.76$ gC/MJ)[44]. $f(T)$ and $f(W)$ describe the effects of air temperature and water, respectively, on the LUE.

$f$(T) is estimated by the equation developed for the Terrestrial Ecosystem Model[45]:

$$f(T) = \frac{(Ta - T_{\min})(Ta - T_{\max})}{(Ta - T_{\min})(Ta - T_{\max}) - (Ta - T_{opt})^2} \quad (7)$$

where, $T_a$ is air temperature; $T_{\min}$, $T_{\max}$, and $T_{opt}$ are the minimum, maximum, and optimal air temperatures of photosynthetic activity, respectively. If the air temperature increases beyond $T_{\max}$ or falls below $T_{\min}$, $f(T)$ is zero.

The water effect is estimated from the satellite-derived LSWI[38, 39]:

$$f(W) = \frac{1 + LSWI}{1 + LSWI_{\max}} \quad (8)$$

where, $LSWI_{\max}$ is the maximum LSWI at individual pixels within the plant growing season.

### 2.4 REG-PEM model performance evaluation

To assess the validity of the model, the GPP estimated from REG-PEM ($GPP_{EST}$) were compared with the GPP predicted from the eddy-covariance tower ($GPP_{EC}$) in a linear regression model. Model agreement was evaluated by the coefficient of determination ($R^2$), the Root Mean Squared Error (*RMSE*), and the Mean

Absolute Error (*MAE*). Here, $R^2$ represents the extent to which variations in the predictions are explained by the model estimation. The *RMSE* and *MAE* quantify the total difference between the estimated and predicted values[46,47].

$$RMSE = \sqrt{\frac{\sum_j^i (GPP_{EST} - GPP_{EC})^2}{j}} \quad (9)$$

$$MAE = \frac{\sum_j^i |GPP_{EST} - GPP_{EC}|}{j} \quad (10)$$

where, $j$ is the total number of observations.

## 3 Results and discussion

### 3.1 Maize GPP estimation and evaluation

The 8-day composite $GPP_{EST}$ values were estimated from the vegetation indices (EVI, LSWI) derived by inputting the MOD09 products and flux tower data into the REG-PEM model. The model sums the daily PAR values over eight days to obtain the 8-day composite PAR and averages the air temperatures over the eight days. The EVI data were smoothed by the HANTS method.

The seasonal dynamics of the $GPP_{EST}$ calculated by the REG-PEM model were compared with the $GPP_{EC}$ and $GPP_{MOD17A2}$ data for 8-day intervals (Figure 2). Both $GPP_{EC}$ and $GPP_{EST}$ exhibited consistent temporal characteristics across all sites and years. The seasonal dynamics (phases and magnitudes) of $GPP_{EST}$ reasonably agreed with those of $GPP_{EC}$. To evaluate whether the REG-PEM model can accurately estimate the maize GPP, a linear regression model was developed between $GPP_{EST}$ and $GPP_{EC}$ values, and the $R^2$, *RMSE* and *MAE* were calculated. The results are listed in Table 2. The correlation coefficient $R^2$ ranged from 0.71 to 0.97, indicating very high correlation between $GPP_{EST}$ and $GPP_{EC}$. The RMSE between $GPP_{EST}$ and $GPP_{EC}$ ranged from 8.12 to 24.78, and the MAE ranged from 4.61 to 17.31.

Maize was continuously cultivated at US-Ne1 station from 2001 to 2004. The phases and magnitudes of $GPP_{EST}$ well agreed with those of $GPP_{EC}$ in 2001 and 2003. However, the $GPP_{EST}$ was underestimated at the heading stage (peak point) in 2002 and 2004, and overestimated during the heading to mature growth stage. In 2004, the $R^2$ between $GPP_{EST}$ and $GPP_{EC}$ was only 0.71, the lowest correlation amongst the study sites.

**Table 2 Statistics between $GPP_{EST}$ and $GPP_{EC}$, and annual total GPP, for the eight study sites**

| Study site | Year | $R^2$ | RMSE | MAE | Total GPP /gC·m$^{-2}$ | | |
|---|---|---|---|---|---|---|---|
| | | | | | $GPP_{EC}$ | $GPP_{EST}$ | $GPP_{MOD17A2}$ |
| US-Ne1 | 2001 | 0.87 | 19.56 | 15.44 | 1316.98 | 1751.74 | 847.78 |
| | 2002 | 0.81 | 18.82 | 12.86 | 1315.76 | 1625.17 | 812.15 |
| | 2003 | 0.85 | 18.09 | 12.64 | 1152.82 | 1721.41 | 810.52 |
| | 2004 | 0.71 | 21.74 | 15.78 | 1148.85 | 1609.89 | 893.73 |
| US-Ne2 | 2001 | 0.91 | 13.33 | 10.79 | 1280.03 | 1403.22 | 697.07 |
| | 2003 | 0.95 | 11.02 | 7.28 | 1374.71 | 1553.49 | 772.36 |
| US-Ne3 | 2001 | 0.87 | 16.78 | 12.52 | 1399.32 | 1444.15 | 668.67 |
| | 2003 | 0.81 | 19.31 | 12.94 | 1160.13 | 1609.82 | 721.44 |
| US-Bo1 | 2001 | 0.92 | 16.53 | 11.04 | 1204.44 | 1550.09 | 826.66 |
| | 2003 | 0.83 | 21.73 | 13.32 | 1495.79 | 1596.55 | 924.74 |
| | 2005 | 0.94 | 12.15 | 8.07 | 1453.81 | 1582.25 | 804.9 |
| US-Bo2 | 2004 | 0.88 | 23.67 | 17.31 | 1821.61 | 1660.37 | 940.07 |
| | 2006 | 0.94 | 11.49 | 8.3 | 1357.9 | 1494.62 | 827.38 |
| US-IB1 | 2006 | 0.97 | 8.12 | 4.61 | 1429.04 | 1390.31 | 820.62 |
| DE-Kli | 2005 | 0.89 | 14.23 | 9.44 | 1366.05 | 1499.5 | 729.08 |
| | 2006 | 0.93 | 11.01 | 6.84 | 1242.45 | 1414.55 | 771.36 |
| YK | 2008 | 0.83 | 17.18 | 11.07 | 1263.07 | 1433.18 | 1041 |
| | 2009 | 0.92 | 24.78 | 12.04 | 1370.86 | 1336.62 | 1104 |

At US-Ne2 and US-Ne3 stations, where maize planting was alternated with soybean planting, the $GPP_{EST}$ and $GPP_{EC}$ were highly consistent over all maize growth stages. The exception was US-Ne2 in 2001, where the model slightly underestimated the GPP in the heading growth stage.

At US-Bo1 and US-Bo2 stations, the heading growth stage was also underestimated in three years. Almost all growth stages were underestimated in 2004 at US-Bo2, and the MAE reached 17.31.

At US-IB1 station, data from only 1 year was suitable for analysis. Although the GPP was slightly underestimated at the beginning of the growth stage, the $R^2$ between $GPP_{EST}$ and $GPP_{EC}$ was the highest among the study sites (0.97). Accordingly, the RMSE and MAE were the lowest amongst the study sites in all years.

At the European station DE-Kli, the $GPP_{EST}$ and $GPP_{EC}$ strongly agreed in 2006, but the REG-PEM model gave an overestimate at the heading stage in 2005. YK station, located in Northwest China, missed parts of the flux data. In this flux tower, the model clearly underestimated the GPP at the heading growth stage in 2008 and 2009. In 2009, the RMSE at this site was the highest among the study sites.

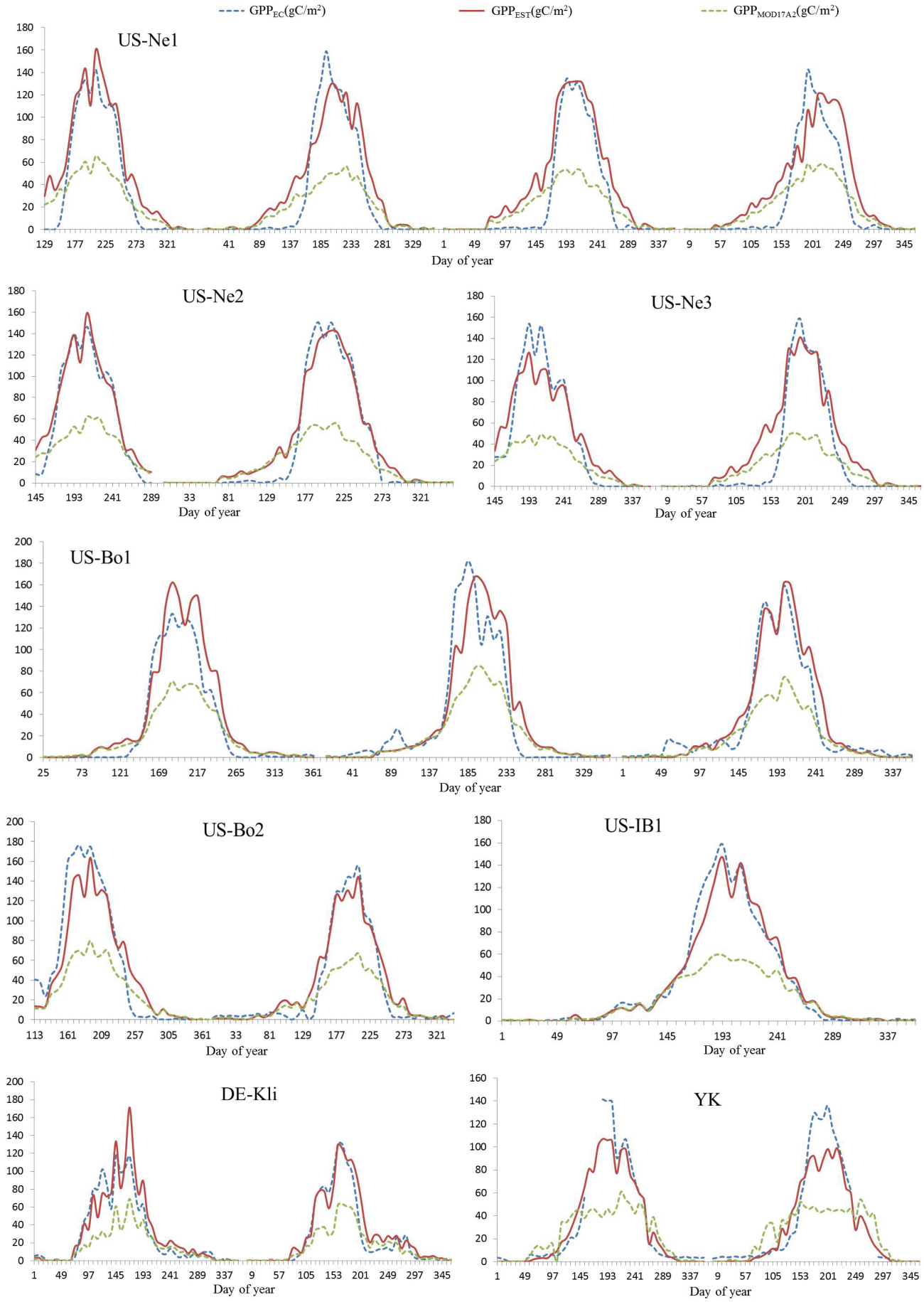


Figure 2 Seasonal dynamics and interannual variation of gross primary production ($GPP_{EST}$, $GPP_{EC}$ and $GPP_{MOD17A2}$) at the eight maize sites

Differences among the study sites were observed in a few 8-day periods. These differences might reflect the sensitivity of the $GPP_{EST}$ to weather data (air temperature or PAR). For example, the REG-PEM predicts higher GPP at higher PAR. In Table 2, there is no obvious evidence that the model results are different among the study sites. Therefore, the REG-PEM model is suitable for maize GPP estimation.

Comparing the $GPP_{EST}$ and $GPP_{EC}$ in Figure 2, we find that the MOD17A2 products obviously underestimate the GPP of maize; in fact, most of the total $GPP_{MOD17A2}$ values were half of their corresponding $GPP_{EST}$ values. Thus, despite being the only global-scale operational GPP product to date, the MOD17A2 products are not readily applicable to maize GPP validation. The maize GPP estimation accuracy is improved by the REG-PEM model.

### 3.2 Uncertainty analysis

Although the phases and magnitudes of the $GPP_{EST}$ and $GPP_{EC}$ were generally well matched, discrepancies were sometimes observed. These discrepancies are attributed partly to estimation error of the $GPP_{EST}$ in the REG-PEM model, and partly to prediction error of the $GPP_{EC}$.

Four parameters are input to the REG-PEM model: PAR, $T_a$, EVI, and LSWI. In this study, the PAR and $T_a$ inputs are the flux tower observations. LUE is considered to cause uncertainty in the main model results[48,49], which is reflected in the spatial heterogeneity and the environmental impact on the remotely sensed data[31]. The maximum LUE is among the most important parameters in the LUE model, as it largely affects the GPP estimation[27]. The differences between field and satellite LUE estimates are most pronounced in croplands[28,50]. Zhang et al.[25] suggested that LUE underestimates are a major cause of GPP underestimation in croplands. In this research, the LUE was assumed constant at 2.76 gC/MJ. However, some studies have estimated the maize GPP through the VPM model, which determines the maximum LUE by linearly or nonlinearly regressing the $CO_2$ flux against the APAR. In site-scale studies, the typical maximum LUE of C4 crops range from 2.40 gC/MJ to 4.24 gC/MJ. In contrast, the maximum LUE of croplands in many large-scale modeling efforts are approximately 0.604-1.08 gC/MJ[28]. In the middle stream of the Heihe River Basin, the maximum LUE value of maize APAR is very high (2.66 gC/MJ[18] versus 2.00 gC/MJ on the Huang-Huai-Hai plain[16]). From flux tower data, Chen et al. determined the maximum LUE of maize as 2.84 ± 0.57 gC/MJ [51].

FPAR is also an important factor in GPP calculations, and can be computed by a wide variety of computational methods. Numerous empirical studies and radiative transfer models have found linear relationships between the FPAR and spectral vegetation indices (e.g., NDVI or EVI). Along with the Leaf Area Index (LAI), the global 8-day FPAR (which is derived from MODIS data by a 3D radiative transfer model) has become a standard land product[52], and the MOD15A2 FPAR forms the basis of MOD17A2 products[53]. Hashimoto et al.[54] analyzed the correlations of short-term and annual flux-measured GPP between MODIS and NDVI, EVI, LAI, and FPAR products. They pointed out that EVI can usefully analyze the short-term variations in site-estimated GPP. Like NDVI, MODIS-FPAR is sensitive to canopy background variations and saturates in areas with dense tree canopies[27], whereas EVI optimizes the canopy background information. Because EVI decouples the canopy background signal and reduces the atmospheric influences[37], it is less sensitive to high biomass than MODIS-PAR and delivers superior vegetation monitoring. Zhang et al.[19] examined the four spectral vegetation indices (VIs) NDVI, EVI, $WDRVI_{green}$ and $CI_{green}$ in daily maize GPP estimates computed by two linear models. Among the four VIs, MODIS EVI performed best in their experiment.

$GPP_{EC}$ also contains uncertainties because it is indirectly derived from the measured net ecosystem exchange and the estimated ecosystem respiration, rather than measured in situ[55,56]. When comparing the tower results and the satellite-based GPP values, the uncertainties in the GPP flux should be considered[22]. The GPP must be computed in two main steps. First, the data gaps must be filled for the NEE; second, the daytime (solar altitude > 0) ecosystem respiration must be estimated. Both of these steps require subjective decisions

and are considerably debated at present[57]. Analyzing a forest site, Dragoni et al.[58] reported the random uncertainty of NEE as 3%-4% of the annual Net Ecosystem Production (NEP). The respiration model is usually based on nighttime measurements when there is no uptake, and predicts the daytime respiration by an assumed relationship between respiration and temperature[59].

## 4 Conclusions

In this research, the GPP of maize at eight study sites was estimated by the REG-PEM model. Comparing the $GPP_{EST}$ and $GPP_{EC}$ values, the GPP estimated by the REG-PEM model well agreed with the GPP predicted by the flux data, demonstrating that MODIS, the flux data and the REG-PEM can potentially estimate the seasonal dynamics and inter-annual variations of the 8-day GPP of maize cropland. This model also predicted the maize GPP with higher accuracy than the MOD17A2 products (which significantly underestimate the GPP of maize croplands). Most of the uncertainty in the REG-PEM model comes from the maximum LUE and the FPAR estimation methods. The result is of significant implications for remote sensing analysis of maize cropland.

## Acknowledgements

We appreciate the flux tower PIs who made these data freely available and all the other people who were involved in the tower field work. We are sincerely grateful to Dr. Conghe Song and Yulong Zhang for their fruitful suggestions. This work was supported by China's Special Funds for Major State Basic Research Project (2013CB733405), the National Natural Science Foundation of China (41471294), the open fund of the State Key Laboratory of Remote Sensing Science (OFSLRSS201408), China Scholarship Council, and OATF from UESTC.

## [References]

[1] Gitelson A A, Viña A, Masek J G, Verma S B, Suyker A E. Synoptic monitoring of gross primary productivity of maize using Landsat data. IEEE Geoscience and Remote Sensing Letters, 2008; 5(2): 133–137.

[2] Cassman K G, Wood S. Cultivated systems. Millennium ecosystem assessment: Global ecosystem assessment report on conditions and trends. Washington D.C.: Island Press. 2005. pp. 741–789.

[3] Beer C, Reichstein M, Tomelleri E, Ciais P, Jung M, Carvalhais N, et al. Terrestrial gross carbon dioxide uptake: Global distribution and covariation with climate. Science, 2010; 329(5993): 834–838.

[4] Wu C, Niu Z, Gao S. Gross primary production estimation from MODIS data with vegetation index and photosynthetically active radiation in maize. Journal of Geophysical Research: Atmospheres, 2010; 115: D12127.

[5] Wu C, Niu Z, Gao S. The potential of the satellite derived green chlorophyll index for estimating midday light use efficiency in maize, coniferous forest and grassland. Ecological Indicators, 2012; 14(1): 66–73.

[6] Malmstrom C M, Thompson M V, Juday G P, Los S O, Randerson J T, Field C B. Interannual variation in global-scale net primary production: Testing model estimates. Global Biogeochemical Cycles, 1997; 11(3): 367–392.

[7] Reeves M C, Zhao M, Running S W. Usefulness and limits of MODIS GPP for estimating wheat yield. International Journal of Remote Sensing, 2005; 26(7): 1403–1421.

[8] Peng Y, Gitelson A A. Application of chlorophyll-related vegetation indices for remote estimation of maize productivity. Agricultural and Forest Meteorology, 2011; 151(9): 1267–1276.

[9] Gitelson A A, Peng Y, Masek J G, Rundquist D C, Verma S, Suyker A, et al. Remote estimation of crop gross primary production with Landsat data. Remote Sensing of Environment, 2012; 121: 404–414.

[10] Peng Y, Gitelson A A, Sakamoto T. Remote estimation of gross primary productivity in crops using MODIS 250 m data. Remote Sensing of Environment, 2013; 128: 186–196.

[11] Sakamoto T, Gitelson A A, Wardlow B D, Verma S B, Suyker A E. Estimating daily gross primary production of maize based only on MODIS WDRVI and shortwave radiation data. Remote Sensing of Environment, 2011; 115: 3091–3101.

[12] Peng Y, Gitelson A A. Remote estimation of gross primary productivity in soybean and maize based on total crop chlorophyll content. Remote Sensing of Environment, 2012; 117: 440–448.

[13] Running S W, Thornton P E, Nemani R, Glassy J M. Global Terrestrial Gross and Net Primary Productivity from the Earth Observing System. In Methods in ecosystem science. New York: Springer-verlag press, 2000. pp.44–57.

[14] Yuan W, Liu S, Zhou G, Zhou G, Tieszen L L, Baldocchi D, et al. Deriving a light use efficiency model from eddy

covariance flux data for predicting daily gross primary production across biomes. Agricultural and Forest Meteorology, 2007; 143(3-4): 189–207.

[15] Kalfas J L, Xiao X, Vanegas D X, Verma S B, Suyker A E. Modeling gross primary production of irrigated and rain-fed maize using MODIS imagery and $CO_2$ flux tower data. Agricultural and Forest Meteorology, 2011; 151(12): 1514–1528.

[16] Yan H, Fu Y, Xiao X, Huang H Q, He H, Ediger L. Modeling gross primary productivity for winter wheat–maize double cropping system using MODIS time series and $CO_2$ eddy flux tower data. Agricultural, Ecosystems and Environment, 2009; 129(4): 391–400.

[17] Wang Z, Xiao X, Yan X. Modeling gross primary production of maize cropland and degraded grassland in northeastern China. Agricultural and Forest Meteorology. 2010; 150(9): 1160–1167.

[18] Wang X, Ma M, Huang G, Veroustraete F, Zhang Z, Song Y, et al. Vegetation primary production estimation at maize and alpine meadow over the Heihe River Basin, China. International Journal of Applied Earth Observation and Geoinformation, 2012; 17(7): 94–101.

[19] Zhang Q, Cheng Y B, Lyapustin A I, Wang Y, Xiao X, Suyker A, et al. Estimation of crop gross primary production (GPP): I. impact of MODIS observation footprint and impact of vegetation BRDF characteristics. Agricultural and Forest Meteorology, 2014; 191(1): 51–63.

[20] Baldocchi D, Falge E, Gu L, Olson R, Hollinger D, Running S, et al. FLUXNET: A new tool to study the temporal and spatial variability of ecosystem-scale carbon dioxide, water vapor, and energy flux densities. Bulletin of the American Meteorological Society, 2001; 82(11): 2415–2434.

[21] Wofsy S C, Goulden M L, Munger J W, Fan S M, Bakwin P S, Daube B C, et al. Net exchange of $CO_2$ in a mid-latitude forest. Science, 1993; 260(5112): 1314– 1317.

[22] Yan H, Wang S Q, Billesbach D, Oechel W, Bohrer G, Meyers T, et al. Improved global simulations of gross primary product based on a new definition of water stress factor and a separate treatment of C3 and C4 plants. Ecological Modelling, 2015; 297: 42–59.

[23] Zhao M, Heinsch F A, Nemani R R, Running S W. Improvements of the MODIS terrestrial gross and net primary production global dataset. Remote Sensing of Environment, 2005; 95(2): 164–176.

[24] Heinsch F A, Zhao M, Running S W, Kimball J S, Nemani R R, Davis K J, et al. Evaluation of remote sensing based terrestrial productivity from MODIS using regional tower eddy flux network observations. IEEE Transactions on Geoscience and Remote Sensing, 2006; 44(7): 1908–1925.

[25] Zhang Y, Yu Q, Jiang J, Tang Y. Calibration of Terra/MODIS gross primary production over an irrigated cropland on the North China Plain and an alpine meadow on the Tibetan Plateau. Global Change Biology, 2008; 14(4): 757–767.

[26] Wang X, Ma M, Li X, Song Y, Tan J, Huang G, et al. Validation of MODIS-GPP product at 10 flux sites in northern China. International Journal of Remote Sensing. 2013; 34(2): 587–599.

[27] Liu Z, Shao Q, Liu J. The performances of MODIS-GPP and -ET products in China and their sensitivity to input data (FPAR/LAI). Remote Sensing, 2015; 7(1): 135–152.

[28] Xin Q, Broich M, Suyker A E, Yu L, Gong P. Multi-scale evaluation of light use efficiency in MODIS gross primary productivity for croplands in the Midwestern United States. Agricultural and Forest Meteorology, 2015; 201: 111–119.

[29] Li S, Niu Z, Yan H, Xu W. Modeling gross primary production in Jiangxi Province using MODIS images. International Conference on Earth Observation Data Processing and Analysis. International Society for Optics and Photonics, 2008: 72854G-72854G-11.

[30] Li S, Hu Z, Liu B, Zhao L, Li, Z. Parameters optimization of remote sensing drived vegetation gross primary production model using ground flux measurement. Sensor Letters, 2012; 10(5-6): 1265–1269.

[31] Li S, Xiao J, Xu W, Yan H. Modelling gross primary production in the Heihe river basin and uncertainty analysis. International Journal of Remote Sensing, 2012; 33(3): 836–847.

[32] Verma S B, Dobermann A, Cassman K G, Walters D T, Knops J M, Arkebauer T J, et al. Annual carbon dioxide exchange in irrigated and rainfed maize-based agroecosystems. Agricultural and Forest Meteorology, 2005; 131(1-2): 77–96.

[33] Wagle P, Xiao X, Suyker A E. Estimation and analysis of gross primary production of soybean under various management practices and drought conditions. ISPRS Journal of Photogrammetry and Remote Sensing, 2015; 99: 70–83.

[34] Gilmanov T G, Aires L, Barcza Z, Baron V S, Belelli L, Beringer J, et al. Productivity, respiration, and light-response parameters of world grassland and agroecosystems derived from flux-tower measurements. Rangeland Ecology and Management, 2010; 63(1): 16–39.

[35] Flerchinger G N, Xaio W, Marks D, Sauer T J, Yu Q. Comparison of algorithms for incoming atmospheric long-wave radiation. Water Resources Research, 2009; 45(3): W03423.

[36] Li X, Li X, Li Z, Ma M, Wang J, Xiao Q, et al. Watershed Allied Telemetry Experimental Research. Journal of Geophysical Research: Atmospheres, 2009; 114: D22103.

[37] Huete A, Didan K, Miura T, Rodriguez E P, Gao X, Ferreira L G. Overview of the radiometric and biophysical performance of the MODIS vegetation indices. Remote Sensing of Environment, 2002; 83(1): 195–213.

[38] Xiao X, Hollinger D, Aber J, Goltz M, Davidson E A, Zhang Q, et al. Satellite-based modeling of gross primary production in an evergreen needleleaf forest. Remote Sensing of Environment, 2004; 89(4): 519–534.

[39] Xiao X, Zhang Q, Braswell B, Urbanski S, Boles S, Wofsy S, et al. Modeling gross primary production of temperate deciduous broadleaf forest using satellite images and climate data. Remote Sensing of Environment, 2004; 91(2): 256–270.

[40] Sakamoto T, Yokozawa M, Toritani H, Shibayama M, Ishitsuka N, Ohno H. A crop phenoogy detecting method using time-series MODIS data. Remote Sensing of Environment, 2005; 96(3): 366–374.

[41] Li S H, Xiao J, Ni P, Zhang J, Wang H, Wang J. Monitoring paddy rice phenology using time series MODIS data over Jiangxi Province, China. International Journal of Agricultural and Biological Engineering, 2014; 7 (6): 28–36.

[42] Roerink G J, Menenti M, Verhoef W. Reconstructing cloudfree NDVI composites using Fourier analysis of time series. International Journal of Remote Sensing, 2000; 21(9): 1911–1917.

[43] Jakubauskas M E, Legates D R, Kastens J H. Harmonic analysis of time-series AVHRR NDVI data. Photogram. Photogrammetric Engineering and Remote Sensing, 2001; 67(4): 461–470.

[44] Prince S D, Goward S N. Global Primary Production: A Remote Sensing Approach. Journal of Biogeography, 1995; 22: 815–835.

[45] Raich J W, Rastetter E B, Melillo J M, Kicklighter D W, Steudler P A, Peterson B J, et al. Potential net primary productivity in South America: application of a global model. Ecological Applications, 1991; 1(4): 399–429.

[46] Liu D, Cai W, Xia J, Dong W, Zhou G, Chen Y. Global validation of a process-based model on vegetation gross primary production using eddy covariance observations. PloS One, 2014; 9(11): e110407.

[47] Wagle P, Xiao X, Torn M S, Cook D R, Matamala R, Fischer M L, et al. Sensitivity of vegetation indices and gross primary production of tallgrass prairie to severe drought. Remote Sensing of Environment, 2014; 152: 1–14.

[48] Gower S T, Kucharik C J, Norman J M. Direct and indirect estimation of leaf area index, fAPAR, and net primary production of terrestrial ecosystems. Remote Sensing of Environment, 1999; 70(1): 29–51.

[49] Ruimy A, Kergoat L, Bondeau A. Comparing global models of terrestrial net primary productivity (NPP): analysis of differences in light absorption and light use efficiency. Global Change Biology, 1999; 5(S1): 56–64.

[50] Garbulsky M F, Peñuelas J, Papale D, Ardö J, Goulden M L, Kiely G, et al. Patterns and controls of the variability of radiation use efficiency and primary productivity across terrestrial ecosystems. Global Ecology and Biogeography, 2010; 19(2): 253–267.

[51] Chen T, van der Werf G R, Gobron N, Moors E J, Dolman A J. Global cropland monthly gross primary production in the year 2000. Biogeosciences, 2014; 11(14): 3871–3880.

[52] Myneni R B, Hoffman S, Knyazikhin Y, Privette J L, Glassy J, Tian Y, et al. Global products of vegetation leaf area and fraction absorbed PAR from year one of MODIS data. Remote Sensing of Environment, 2002; 83(1): 214–231.

[53] Song C, Dannenberg M P, Hwang T. Optical remote sensing of terrestrial ecosystem primary productivity. Progress in Physical Geography, 2013; 37(6): 834–854.

[54] Hashimoto H, Wang W, Milesi C, White M A, Ganguly S, Gamo M, et al. Exploring Simple Algorithms for Estimating Gross Primary Production in Forested Areas from Satellite Data. Remote Sensing, 2012; 4(1): 303–326.

[55] Zhang Y, Song C, Sun G, Band L E, Noormets A, Zhang Q. Understanding moisture stress on light use efficiency across terrestrial ecosystems based on global flux and remote‐sensing data. Journal of Geophysical Research: Biogeosciences, 2015; 120(10): 2053–2066.

[56] Reichstein M, Falge E, Baldocchi D, Papale D, Aubinet M, Berbigier P, et al. On the separation of net ecosystem exchange into assimilation and ecosystem respiration: Review and improved algorithm. Global Change Biology, 2005; 11(9): 1424–1439.

[57] Falge E, Baldocchi D, Tenhunen J, Aubinet M, Bakwin P, Berbigier P, et al. Seasonality of ecosystem respiration and gross primary production as derived from FLUXNET measurements. Agricultural and Forest Meteorology, 2002; 113(1): 53–74.

[58] Dragoni D, Schmid H P, Grimmond C S B, Loescher H W. Uncertainty of annual net ecosystem productivity estimated using eddy covariance flux measurements. Journal of Geophysical Research: Atmospheres, 2007; 112:D17102.

[59] Falge E, Baldocchi D, Olson R, Anthoni P, Aubinet M, Bernhofer C, et al. Gap filling strategies for defensible annual sums of net ecosystem exchange. Agricultural and Forest Meteorology, 2001; 107(1): 43–69.